

Models for ultraviolet radiation–dependent photoinhibition of Lake Erie phytoplankton

Véronique P. Hiriart-Baer¹ and Ralph E. H. Smith

Department of Biology, University of Waterloo, Waterloo, Ontario, N2L 3G1 Canada

Abstract

We calibrated a model for ultraviolet radiation (UVR) and photosynthetically active radiation–dependent photoinhibition, with explicit damage and recovery processes (the *R* model), against observations of photosynthesis by Lake Erie phytoplankton exposed to natural sunlight in the summer of 1998. The model explained 74%–96% of the variation in photosynthetic rates and indicated active recovery processes at 4 of the 5 experimental stations. UVR-dependent photoinhibition kinetics were not as well explained by two simpler models that assumed either a lack of recovery processes or an instantaneous equilibrium between damage and recovery. The 1998-calibrated *R* model also provided consistently significant predictions of photoinhibition in 10 experiments done the previous year, albeit with a reduced goodness-of-fit, whereas simpler models did not. Biological weighting functions (BWFs) derived for UVR effects in 1998 were similar in shape throughout the UVR part of the spectrum, with an especially steep decrease from 300 to 320 nm, compared with BWFs published for other phytoplankton communities and/or species. The *R* model predicted photoinhibitory losses of primary production, integrated through the photic zone, that were intermediate between the two simpler models and showed that Lake Erie phytoplankton varied in both their spectral sensitivity (as expressed by the BWF) and recovery rates.

Much research has been done in recent years on the implications of diminished stratospheric ozone concentrations, and the associated increases in surface-incident ultraviolet radiation (UVR), on phytoplankton primary production by phytoplankton (e.g., Smith et al. 1992; Prezelin et al. 1994; Neale et al. 1998*b,c*). Moreover, there is growing concern of the potential effects of climate change on colored dissolved organic matter, which is composed of compounds that are known to play a significant role in UVR attenuation (Pienitz and Vincent 2000). It has not been easy to develop fully satisfactory estimates of the effects of UVR on primary production, partly because UVR belongs to a continuous solar radiation spectrum that acts both beneficially and detrimentally on photosynthesizing organisms. Solar radiation drives the photosynthetic conversion of inorganic carbon to organic substrates, yet excessive visible light, as well as UVR, can inhibit photosynthesis (Cullen and Lesser 1991; Villafañe et al. 1995), damage intracellular components such as DNA (Karentz et al. 1991; Prézélin et al. 1994), and inactivate certain key photosynthetic proteins (Greenberg et al. 1989; Wilson et al. 1995). Another major complication in assessing the effects of UVR on plankton is the natural variability in exposure regime that is associated with vertical mixing processes (Smith and Cullen 1995).

Phytoplankton have evolved a variety of mechanisms to prevent or counteract the damage from UVR and excessive

light, such as DNA photoreactivation, the synthesis of photoprotective pigments, and dark repair processes (Karentz 1999; Roy 2000). Although the timescales of photoinhibition vary on the order of minutes to hours, some photoprotection measures occur within seconds or minutes (e.g., energy dissipation via fluorescence, state transitions, or nonradiative decay), and others occur on the order of hours to days (e.g., synthesis of protective pigments, or chemical quenchers; Ferris and Christian 1991; Villafañe et al. 1995). The kinetics of these processes are important when the timescales of vertical water column mixing, and, thus, radiation exposure, are considered, and they can be influenced by factors such as nutrient availability and species composition (Karentz et al. 1991; Lesser et al. 1994; Xiong et al. 1997). Finite, but variable, kinetics of both photodamage and recovery processes in phytoplankton communities can therefore be anticipated.

Photoinhibition by UVR is wavelength-specific because of the variation of photon energies and intracellular targets of action across the UVR waveband. Action spectra, which are derived through near-monochromatic exposures, are useful for identifying sites and mechanisms of photoinhibition, but polychromatic exposures are more realistic when the questions concern the effect of UVR in natural systems (Coohill 1997). The value of the polychromatic approach is that the longer ultraviolet A (UVA) and short visible wavelengths play an active role in photoenzymatic repair (Mitchell and Karentz 1993; Roy 2000), which may be important in mitigating the effects of the shorter ultraviolet B (UVB) wavelengths. However, UVA and visible light can also be inhibitory (e.g., Herrmann et al. 1997) and may reinforce some of the indirect modes of UVB impact, such as damage from reactive oxygen species (Vincent and Neale 2000). The final effect on the target organisms therefore reflects interactions among different parts of the incident spectrum and is best reflected in a biological weighting function (BWF) derived from realistic polychromatic exposures (Neale 2000). BWFs are essential for estimating the effect of UVR on primary

¹ Corresponding author (vphiriar@sciborg.uwaterloo.ca).

Acknowledgments

We thank Technical Operations and the officers and crew of CCGS *Limnos*, who provided valuable assistance in the field, and Murray Charlton of the National Water Research Institute. We also thank Dr. P. J. Neale and an anonymous reviewer for their input and suggestions, which significantly improved the quality of the manuscript.

This research was supported by the National Sciences and Engineering Research Council (R.S.), Environment Canada (R.S.), and the International Association of Great Lakes Research (C.S. Mott scholarship to V.H.-B.).

production in vertically mixed systems, where phytoplankton cells often experience large variations in spectral irradiance on timescales of minutes to hours (e.g., Cullen et al. 1992; Neale et al. 1998b).

Although some researchers have proposed that photoinhibition is a simple linear function of biologically weighted UVR exposure (e.g., Behrenfeld et al. 1993; Boucher and Prézelin 1996), there is no mechanistic basis for such relationships, and there is every reason to expect nonlinear functions instead (Cullen and Neale 1997). A more realistic, although still simple, model postulates that photoinhibition is essentially a reversible conversion between functional and nonfunctional states that leads to nonlinear, but tractable, predictive equations for certain limiting cases (Neale 2000). In one limiting case, damage and recovery are in equilibrium because the kinetics of both processes are very rapid (the irradiance-dependent model; Cullen et al. 1992). Alternatively, recovery may be essentially inactive, so that photoinhibition is a function solely of accumulated damage (the cumulative exposure model; Neale et al. 1998b).

Both limiting cases of the two-state model have had success in describing UVR-dependent photoinhibition in different applications (Cullen et al. 1992; Lesser et al. 1994; Neale et al. 1998b). The irradiance-dependent model has correctly described the photoinhibition of algae fully acclimated to the prevailing UVR regime, as has best been seen in studies of laboratory cultures (Cullen et al. 1992; Lesser et al. 1994). The cumulative exposure model, on the other hand, has successfully described the response of natural communities, particularly those encountered under conditions of deep vertical mixing (and presumably low average light exposure) and/or low temperatures (Neale et al. 1998b, 2001a; Smith et al. 1998). Neither model has been successful in application to all situations.

Here we present measurements of the kinetics of UVR-dependent photoinhibition in Lake Erie phytoplankton in 1997 and 1998. We compared the irradiance-dependent and cumulative-exposure models to a more complicated model that allows for finite rates of recovery without assuming the instantaneous equilibration between damage and recovery, and we estimated BWFs to describe the spectral variation of inhibitory power of natural sunlight. The results support the idea that recovery is an active, but variable, process in natural phytoplankton communities and that it requires the more complicated model for accurate description. The results also suggest, however, that simpler and more tractable models could provide useful approximations for modeling photoinhibitory losses throughout the photic zone.

Materials and methods

Study sites—Lake Erie displays consistent east-west spatial gradients. The west basin is shallow (mean depth, 7.3 m), turbid (the diffuse vertical attenuation coefficient, K_{dPAR} , averages 0.80 m^{-1} in summer) and mesotrophic (average total P of $23\text{ }\mu\text{g P L}^{-1}$ from spring through summer; Charlton et al. 1999; Hiriart et al. 2002; R. Smith unpubl. data). The central and eastern basins are progressively deeper (mean depth, 18 and 24 m, respectively), clearer (K_{dPAR} averaging

0.4 and 0.3 m^{-1}) and more oligotrophic (total P averaging 11 and $10\text{ }\mu\text{g P L}^{-1}$). Sampling and field experiments were conducted at stations in all three basins (Fig. 1, Table 1). The sampling regimen did not permit a well-controlled comparison among basins but did allow us to assess phytoplankton responses in samples from a range of limnological conditions. Experiments were conducted with samples from 10 stations in 1997, between the months of May and August, but the radiation exposure design did not permit the derivation of BWFs. The more elaborate design used at five stations in June, July, and August of 1998 did permit the derivation of BWFs and thorough testing of the *R* model.

Experimental procedures—Experiments were conducted on the CCGS *Limnos* under relatively clear sky conditions. The physical structure of each lake station was measured by conductivity, temperature, and depth sensors (SBE-25 models, EBTT and Water Quality Profiler, SeaBird Electronics), and a SeaBird SBE-19 equipped with a SeaTech fluorometer cast characterized the in vivo chlorophyll *a* fluorescence profiles. Incident solar radiation spectra were measured with a diode-array spectroradiometer (Oriel) equipped with a collecting sphere at 0.5-nm intervals from 295 to 700 nm every 30 min (Smith et al. 1999). In practice, little measurable radiation was found at the lower end of the measured spectrum, so our UVB measurements were quantified as the amount of radiation between 297 and 320 nm. The radiometer was calibrated with a lamp traceable to the National Bureau of Standards specifications, and wavelength calibration was done with reference to known absorption lines in the incident solar spectrum. The underwater photosynthetically active radiation (PAR) regime was characterized using a LI-COR LI-1000 with an underwater cosine quantum sensor to determine diffuse attenuation coefficients (PAR only) and the mean PAR within the mixed layer.

Whole-water samples for onboard experiments were taken early in the morning at 5 m depth (except 1 July 1997, when water sample taken from 3 m) with Niskin bottles so that the incubations could begin by 1000 h. Samples were kept in the dark for ~ 2 h until the beginning of each experiment. In these time-series experiments, all reported photosynthetic rates are means of triplicates from independent incubation vessels. Lake water samples were inoculated with ^{14}C -sodium bicarbonate (ICN Biomedicals; 0.074 Bq L^{-1}) and dispensed into acid-washed quartz tubes (55 ml) or polystyrene flasks (65 ml; 1997 only). The incubation vessels were then placed in UVR-transmitting plexiglass deck boxes fitted with different optical filters and sampled at preestablished time intervals. In 1997, quartz tubes were sampled after 0.5, 1, 2, 4, 6, and 8 h of exposure, and polystyrene flasks were sampled after 1, 3, and 8 h of exposure. In 1998, the quartz tubes were sampled at 0.5, 1, 2, and 4 h of exposure, when possible.

At each sampling time and at time 0, a 5-ml subsample from each experimental vessel was acidified with $100\text{ }\mu\text{l}$ of 6 N HCl, and then fixed after 24 h with 15 ml of EcoLume scintillation cocktail (ICN Pharmaceuticals). Total activity ($200\text{ }\mu\text{l}$) samples were also taken, to verify the isotope additions. Photosynthetic carbon assimilation was calculated using dissolved inorganic carbon concentrations measured

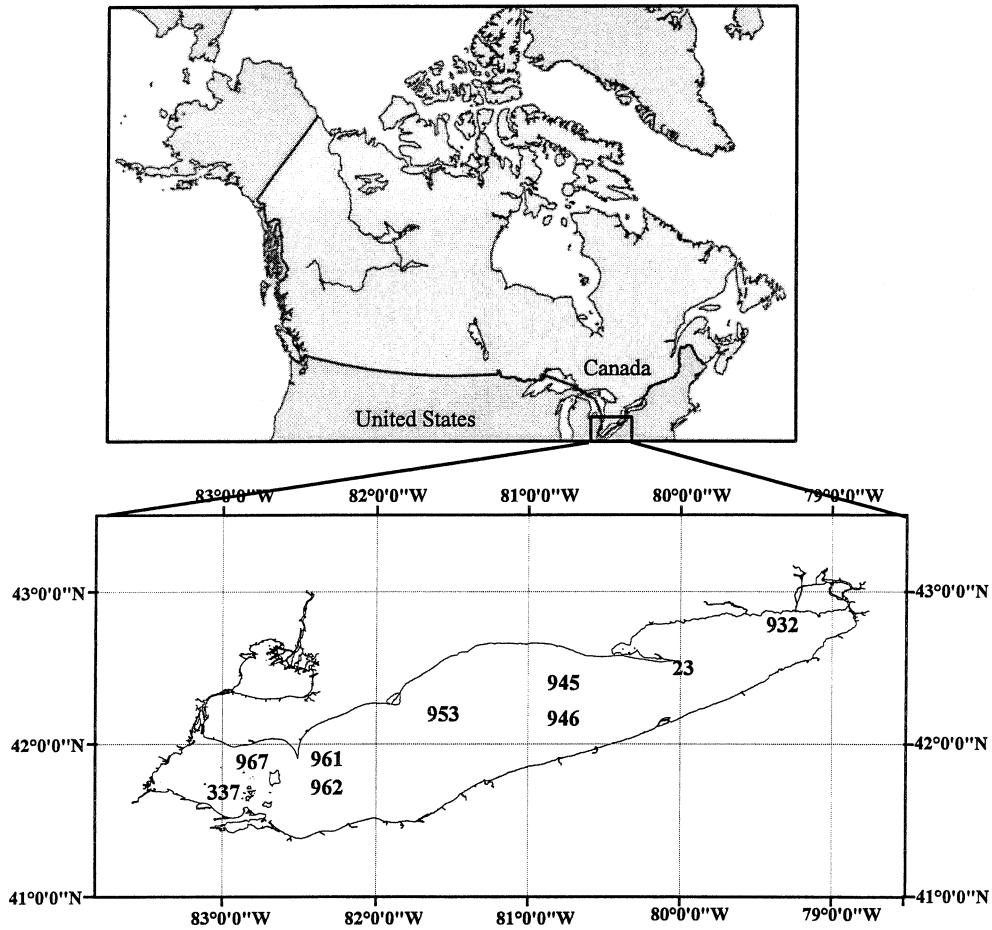


Fig. 1. Lake Erie and the lake stations sampled throughout the summers of 1997 and 1998.

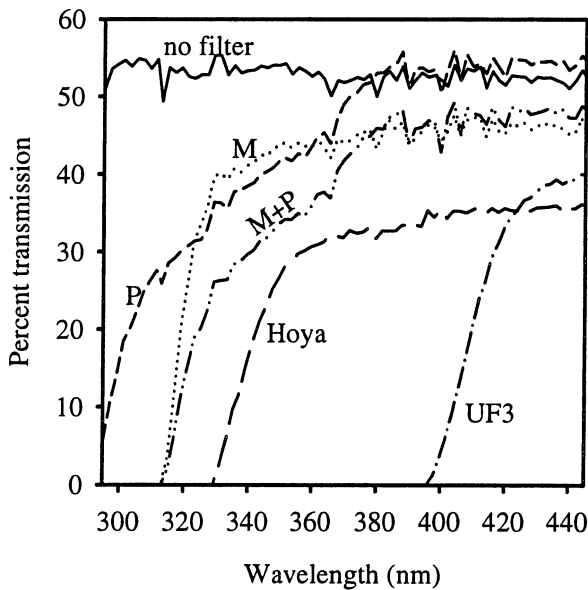


Fig. 2. Percentage transmission of UV wavelengths for the different 50% PAR spectral treatments. M = Mylar-D filter; P = polystyrene filter; M+P = Mylar-D and polystyrene filters; Hoya = Hoya UV340 glass filter; UF3 = total UVR filter.

on filtered (glass fiber; GF/F) lake water from each station. Initial total Chl *a* concentration was measured by fluorometry (e.g., Smith et al. 1999) and phytoplankton community composition by microscopic examination of samples preserved with Lugol's iodine.

The various treatment exposures were achieved using different optical filters and supplemental UVB lamps. In 1997, different combinations of filters and two different experimental vessels (quartz tubes and polystyrene flasks) yielded a total of eight treatments with two levels of irradiance (100% and 50% PAR) and four (100%, 50%, 30%, and 15% UVB exposure levels) different spectral qualities. In 1998, only quartz tubes were used as the experimental vessels, and polystyrene sleeves were used as an optical filter. These conditions, in addition to a Hoya glass filter and the use of supplemental UVB lamps, yielded a total of 10 treatments with two levels of irradiance (100% and 50% PAR), and seven different spectral quality treatments were used (Fig. 2). All treatments were used on 9 June, 14 July, and 12 August. On 8 June and 13 August, no supplemental UVB lamps were used. On 13 August, UF3 filter treatments were excluded. Table 2 lists the approximate waveband ratios for each treatment in 1998.

The photosynthetic parameters (P_m^b and α^b) were estimated with a light gradient incubator (nine irradiances, 0.4 to

Table 1. Summary of limnological variables of the stations sampled for time-series experiments conducted on Lake Erie between May and August 1997 and June and August 1998. The mean PAR is the average light climate within the mixed layer. E, east basin; C, central basin; W, western basin.

Date	Sta.	Basin	Mix depth (m)	Temperature (°C)	Chl <i>a</i> (μg L ⁻¹)	<i>K_d</i> _{PAR} (m ⁻¹)	Mean PAR (% of incident)
7 May 1997	946	C	22*	6.0	1.5	0.43	10.6
3 Jun 1997	946	C	22*	8.8	2.5	0.29	15.1
4 Jun 1997	337	W	9*	13.2	9.8	1.61	6.9
5 Jun 1997	961	C	19*	13.4	1.2	0.83‡	6.3
1 Jul 1997	23	E	5*	20.3	0.7	0.36	46.4
2 Jul 1997	967	W	8.5	23.5	2.1	0.36	32.8
29 Jul 1997	23	E	15	22.0	3.5†	0.24	27.0
30 Jul 1997	953	C	12	22.2	1.4	0.32	25.5
31 Jul 1997	962	C	11	23.7	2.0	0.36‡	24.8
27 Aug 1997	337	W	9*	21.1	15.5	1.16	9.6
8 Jun 1998	932	E	21*	15.0	1.3	0.19	24.6
9 Jun 1998	945	C	10	12.8	2.3	0.27	34.5
14 Jul 1998	946	C	15	22.5	1.1	0.19	33.1
12 Aug 1998	337	W	9*	24.8	4.7	0.63	17.6
13 Aug 1998	961	C	9	22.5	3.1	0.23†	42.2

* On these dates, the water columns were isothermal.

† In vivo chlorophyll fluorescence was not uniformly distributed within the mixed layer on this date.

‡ Derived from the following relationship: $K_{dPAR} = -0.026 \times \text{transmission} + 2.258$.

~2000 μmol m⁻² s⁻¹ PAR only) using the model of Platt et al. (1980). At no time was photoinhibition a significant contributor to the photosynthesis versus light (P-E) relationship in these short (1-h) incubations. The Platt et al. (1980) model was therefore fitted without the photoinhibition term.

Photoinhibition models—Fundamentally, photosynthetic rates are assumed to be proportional to the irradiance of PAR. This basic relationship can be modified through photoinhibition from excessive PAR and/or the more photoreactive UVR. Photosynthesis in the presence of inhibiting radiation should often reflect both damage and recovery processes, which vary with exposure (UVR and PAR) and physiological condition. The relationship between optimal photosynthesis and the damage and recovery processes can most simply be represented as

Table 2. Radiation treatments used in primary production experiments, with all treatments exposed to direct natural sunlight. Waveband ratios are presented as relative to the PAR incident spectra. These were calculated from actual radiation transmission across each spectral treatment.

Neutral density filter (% transmission)	Spectral treatment manipulation (lamp and/or filter)	Approximate ratio of UVB:UVA:PAR
100 or 50	UF3 acrylic filter	0.0:0.0:93
100 or 50	No lamp or filter	1.0:10:100
100 or 50	Mylar-D filter	0.1:8.1:88
50 only	Polystyrene filter	0.2:4.7:55
50 only	Polystyrene + Mylar-D filter	0.0:3.8:49
50 only	Hoya UV340 glass filter	0.0:3.6:48
50 only	UVB lamp + cellulose acetate	0.6:6.2:6.1

$$\frac{dP_{(t)}}{dt} = -k_1 E_{inh}^* P_{(t)} + k_2 (1 - P_{(t)}) \quad (1)$$

where $P_{(t)}$ is the photosynthetic rate normalized to an optimal rate (P/P_{opt}) at time t , k_1 , and k_2 are the damage and recovery rate constants, and E_{inh}^* is the biologically weighted inhibitory irradiance. The first term on the right-hand side of Eq. 1 describes the damage kinetics, whereas the second term describes the recovery kinetics. We call Eq. 1 the *R* model because it allows for finite recovery rates.

The irradiance-dependent (*E*) model (Cullen et al. 1992) is a simplification of Eq. 1 that assumes that the rate of change of photosynthesis over time, relative to the rate obtained in the absence of photoinhibition, is zero (i.e., $\partial P_{(t)}/\partial t = 0$) because k_1 and k_2 are large, which results in a near-instantaneous equilibrium. The cumulative exposure (*H*) model (Neale et al. 1998b), on the other hand, simplifies Eq. 1 by assuming that $k_2 = 0$, so the kinetics of photoinhibition are strictly a function of exposure. In some situations, however, neither assumption may be justifiable (Neale 2000).

Fitting models—The models were fitted, and BWFs were statistically estimated for each 1998 sample, according to the method described by Cullen and Neale (1997). In brief, the UVR spectral irradiances, at 2-nm wavelength intervals, were normalized to E_{PAR} (W m⁻²), and principal components analysis (PCA) was done to derive the principal components (PCs) representative of the original spectral shape of the various spectral treatments. Coefficients of influence (m_k ; (J m⁻²)⁻¹) and component scores ($c_{i,k}$; dimensionless) for each PC were estimated by nonlinear regression. For the *R* model, the model statement was

$$\frac{P_{avg}}{P_{opt}} = \frac{A}{(A + k_2)^2 T} [1 - e^{-(A+k_2)T}] + \frac{k_2}{A + k_2} \quad (2)$$

where

Table 3. Summary of the statistical analysis of algal photoinhibition, using the repair model, for Lake Erie phytoplankton. The maximum solar PAR ($E_{\text{PAR(max)}}$; $\mu\text{mol m}^{-2} \text{s}^{-1}$) is supplied for exposure comparisons between dates. Photosynthetic parameters, maximum photosynthetic rates (P_m^b ; $\mu\text{g C } \mu\text{g Chl}^{-1} \text{h}^{-1}$) are the fitted values \pm the asymptotic SE of the estimate, and the light saturation parameter (E_k ; $\mu\text{mol m}^{-2} \text{s}^{-1}$) values were calculated as P_m^b/α^b from the P vs. E curves and are reported here as indicators of light adaptations status. Model parameters listed are $\epsilon_{R(300)}$ [J m^{-2}] $^{-1}$] represent the biological effectiveness coefficient values at 300 nm, and k_2 is the estimated recovery constant (s^{-1}) fitted by the R model (see "Materials and Methods") with the total number of observations used in the fitting included in parentheses, respectively.

Date	Dominant genera of nano- and microphytoplankton	$E_{\text{PAR(max)}}$	P_m^b	E_k	$\epsilon_{R(300)}$	r^2	$k_2 \times 10^{-4}$
8 Jun 1998	<i>Ochromonas</i>	1026	5.91 ± 0.20	227	1.08	0.957	$0.014 \pm 0.09_{(27)}$
9 Jun 1998	<i>Ochromonas/Asterionella</i>	576	3.72 ± 0.16	169	9.32	0.915	$4.28 \pm 0.31_{(40)}$
14 Jul 1998	<i>Franceia/Dinobryon/Anabaenopsis</i>	687	2.18 ± 0.10	37.6	16.1	0.922	$3.99 \pm 0.28_{(40)}$
12 Aug 1998	<i>Aphanothece/Selenastrum</i>	875	4.76 ± 0.23	144	1.41	0.735	$6.54 \pm 0.76_{(40)}$
13 Aug 1998	<i>Cyclotella/Aphanothece</i>	731	2.11 ± 0.10	84.4	40.4	0.768	$18.25 \pm 1.72_{(21)}$

$$A = E_{\text{PAR}_i} \left(m_0 + \sum_{k=1}^z m_k c_{i,k} \right) \quad (3)$$

where $P_{\text{avg}}/P_{\text{opt}}$ (dimensionless) is cumulative photosynthesis relative to optimal cumulative photosynthesis in the absence of photoinhibition obtained from the independent P-E curves, k_2 is the estimated recovery rate constant, T is the exposure period, m_0 is the coefficient of influence for the mean spectrum plus PAR, and m_k is the coefficient of influence for each PC included in the analyses. The number of PCs needed to derive the different BWFs, z , was determined by partial F test (Cullen and Neale 1997). The biological effectiveness coefficients ($\epsilon_R(\lambda)$ in J m^{-2}) $^{-1}$) at each wavelength were then calculated as

$$\epsilon_R(\lambda) = \frac{\sum_{k=1}^z m_k w_k(\lambda)}{\text{SD}[E_N(\lambda)]} \quad (4)$$

where w_k is the component weighting and E_N is the normalized UVR spectral irradiance. The standard error of the effectiveness coefficients at each wavelength was calculated using error propagation (Cullen and Neale 1997). The E and H models were fitted to their respective, and simpler, model statements (Eqs. 5, 6), and BWFs were derived similarly.

Model extrapolations—All three models were also fitted to the 1997 data, which were insufficient to allow the derivation of BWFs, by applying BWFs derived in 1998. In practice, the irradiance (E) model was fitted as

$$\frac{P}{P_{\text{opt}}} = \frac{1}{1 + a \cdot E_{\text{UVR}}^*} \quad (5)$$

where E_{UVR}^* (dimensionless) is UVR irradiance ($\text{W m}^{-2} \text{nm}^{-1}$) weighted by the appropriate BWF and summed over all wavelengths. The coefficient a (dimensionless) allows for variations in overall sensitivity of the phytoplankton while assuming that the shape of the BWF is appropriate. The cumulative exposure (H) model was fitted as

$$\frac{P_{\text{avg}}}{P_{\text{opt}}} = \frac{1 - e^{-a \cdot T \cdot E_{\text{UVR}}^*}}{a \cdot T \cdot E_{\text{UVR}}^*} \quad (6)$$

where E_{UVR}^* is UVR irradiance weighted as above but aver-

aged over the exposure period T , and the coefficient a is dimensionless. The R model was fitted to observations of $P_{\text{avg}}/P_{\text{opt}}$ and weighted relative irradiances as in Eq. 2, and A was

$$A = aE_{\text{UVR}}^* \quad (7)$$

All statistical analyses were done using Systat (version 7.0; SPSS).

Modeling integrated photoinhibitory losses—Using the modeling package Stella (version 5.1.1 for Windows), the vertically integrated inhibition of primary production was calculated with each model, using their respective BWFs. The purpose was to estimate the loss of production during a typical summer day for three algal communities with varying responses to UVR (8 June, 14 July, and 12 August 1998) and to determine whether choice of model influenced the estimates of photoinhibitory losses.

Photoinhibition was modeled for each algal community using their respective photosynthetic parameter values (P_m^b and α^b). A representative, sunny day, diurnal radiation spectrum (4 June 1997) with measurements at 20-min intervals (0940 to 1920 h) was used. Although summer days can be as long as 16 h, the 10-h photoperiod modeled here was centered around the maximum UVR photoperiod and would include most of the inhibitory part of the photoperiod. We assumed a 10-m mixed depth and an organized water motion (Langmuir circulation) with moderate and fast mixing rates (5- and 0.5-h cycle $^{-1}$).

Integrated primary production was calculated for the 10-h photoperiod by predicting relative photosynthetic rates at 15-min intervals, according to the kinetic model, and calculating cumulative photosynthesis. Relative inhibition was calculated by comparing predicted photosynthesis using the full spectrum to an optimum calculated from just P_m^b and α^b —that is, no photoinhibition attributed to PAR. This was done for 51 theoretical algal cells either remaining at one point within the water column for the entire photoperiod or phytoplankton cycling at different rates and starting the day at different depths within a $\frac{1}{2}$ Langmuir cell. We assumed that the UVR sensitivity (BWF) and the specific rate of recovery remained constant throughout the day and that the algal biomass was uniformly distributed within the water column.

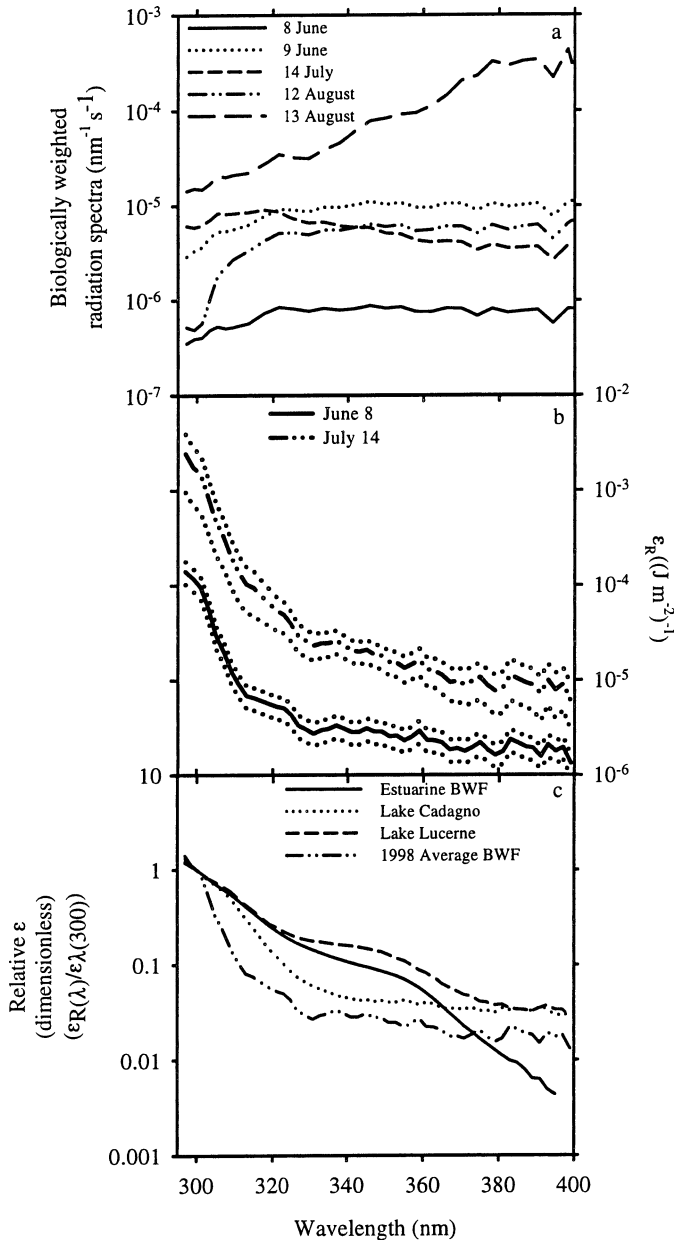


Fig. 3. BWFs derived from PCA using the R kinetic model for the 1998 experimental dates. (A) Biologically weighted radiation spectra for each 1998 BWF, the cross-product ($\text{nm}^{-1} \text{s}^{-1}$) of the biological effectiveness coefficients, and a representative incident radiation spectra. The sum of the cross-product—the indicator of overall UVR sensitivity—for each BWF is $0.07 \times 10^{-3} \text{ s}^{-1}$, $0.90 \times 10^{-3} \text{ s}^{-1}$, $0.56 \times 10^{-3} \text{ s}^{-1}$, $0.50 \times 10^{-3} \text{ s}^{-1}$, and $13.1 \times 10^{-3} \text{ s}^{-1}$ for 8 June, 9 June, 14 July, 12 August, and 13 August 1998, respectively. (B) Absolute values of the effectiveness coefficients with 95% confidence intervals (dotted lines) for two of the BWFs derived: 8 June and 14 July 1998. (C) Relative weighting coefficients for a calculated average 1998 BWF normalized to the $\epsilon_{R(300)}$ value. Three BWFs from the literature are graphed for comparison: an average BWF for estuarine phytoplankton (Banaszak and Neale 2001) and BWFs from two Swiss lakes, Lake Cadagno (mesotrophic, shallow [$z_{\text{max}} = 20 \text{ m}$], meromictic alpine freshwater lake) and Lake Lucerne (oligotrophic, deep [mean $z = 104 \text{ m}$], holomictic, prealpine freshwater lake) (Neale et al. 2001b).

PAR was modeled using the median attenuation coefficient determined in lakewide surveys in 1997 (0.26 m^{-1}). UVR was modeled using wavelength-specific attenuation coefficients ($K_{d\lambda}$) predicted from relationships in Smith et al. (1999) for median conditions of PAR transparency ($K_{d\text{PAR}}$) and total suspended solids. Radiation at each depth interval was calculated with incident spectral radiation weighted with the BWF derived from the algal assemblage sampled on each respective date. The experiments conducted on 8 June, 14 July, and 12 August 1998 were chosen for their $\lambda_{R(300)}$ and k_2 values, which yielded three very different scenarios: (1) low sensitivity (i.e., $\lambda_{R(300)}$) and low recovery rate (k_2) (8 June 1998), (2) high sensitivity and high recovery rate (14 July 1998), and (3) low sensitivity and high recovery rate (12 August 1998).

Results

Limnological conditions—The limnological conditions found at the experimental stations are listed in Table 1; limnological measurements, but no experiments, were done at many additional stations. On the basis of 134 (1997) or 111 (1998) profiles, strong and probably persistent ($>1^\circ \text{C m}^{-1}$) thermoclines were found regularly only in the east and central basins, in July and August. Of the experimental stations used in 1997, only the July stations showed clear signs of persistent thermal stratification. Of the five experimental stations in 1998, only the central basin stations showed signs of persistent stratification.

The in vivo fluorescence profiles of the experimental stations showed that the water samples collected at 5 m were representative of the mixed layer except for Sta. 23 (29 July 1997) and Sta. 945 and 946 (9 June and 14 July 1998), where chlorophyll increased with depth in the top 10 m of the water column. Subsurface chlorophyll maxima were observed at some stations, including Sta. 945 (9 June 1998). All subsurface chlorophyll peaks occurred in or near the main thermocline. Although variable, chlorophyll concentrations were higher, on average, in the west basin ($8.0 \pm 7.9 \mu\text{g L}^{-1}$) than in the east and central basins (1.8 ± 1.4 and $1.9 \pm 0.5 \mu\text{g L}^{-1}$).

BWFs—All of the BWFs derived for Lake Erie phytoplankton showed significant inhibitory effects of both UVB and UVA, although the weightings at each wavelength varied between experimental dates (Fig. 3). We calculated the biologically effective radiation spectrum (B_{eff}) corresponding to each BWF (Fig. 3a), to compare the variations of impact across the solar spectrum between the different experimental dates. The algal assemblage sampled on 8 June 1998 demonstrated relatively low sensitivity, whereas the sample from 13 August 1998 demonstrated a significantly higher sensitivity, particularly to the longer UVA wavelengths (360–400 nm). The other sampling dates revealed algal communities with intermediate sensitivity.

When normalized to the $\epsilon_{R(300)}$ values, the BWFs (except that for 13 August 1998) showed similarities in shape, despite variations in absolute values, with relatively high sensitivity to the shorter UVB wavelengths and low sensitivity to the longer UVA wavelengths. The average BWF (exclud-

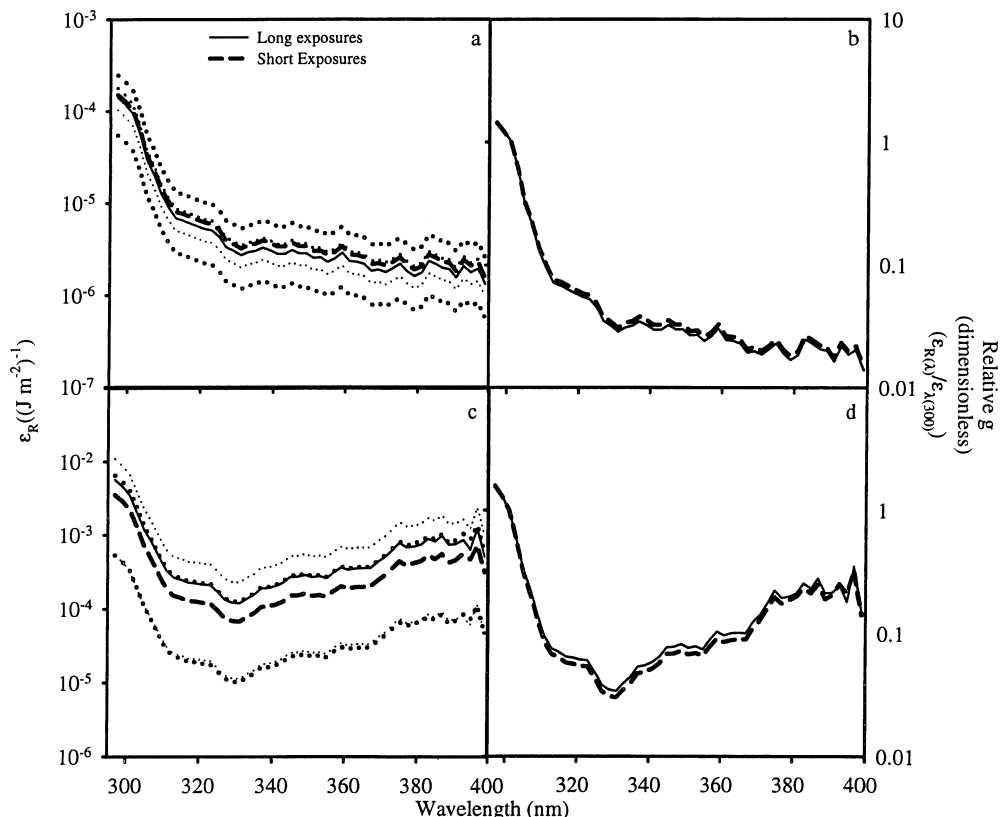


Fig. 4. Comparison of the BWFs derived using only the short exposures (≤ 1 h) and using the entire time-series data set for 8 June and 13 August 1998. (A) 8 June 1998 BWF absolute effectiveness coefficient values with 95% confidence intervals for both the short (thick dotted line) and long (thin dotted lines) exposures. (B) 8 June 1998 short and long normalized effectiveness coefficients. (C) 13 August 1998 BWF absolute effectiveness coefficient values with 95% confidence intervals for both the short (thick dotted lines) and long (thin dotted lines) exposures. (D) 13 August 1998 short and long normalized effectiveness coefficients.

ing that from 13 August 1998) was compared with previously published BWFs for marine and freshwater phytoplankton (Fig. 3c). Collectively, the BWFs reveal considerable variation in shape. However, the average Lake Erie BWF was distinguished by distinctly lower normalized weighting coefficients from 305 to 360 nm.

BWFs were also derived by fitting the R model to the shorter exposure (i.e., ≤ 1 h) data only (Fig. 4). The absolute values of the effectiveness coefficients ($\lambda_{R(\lambda)}$) of the 1-h BWF were not significantly different from those of the 4-h BWF. When normalized to 300 nm, the shapes of the 1- and 4-h BWFs were almost identical, except for that from 14 July 1998 (Fig. 4c). On that date, the 1-h normalized spectra revealed higher relative effectiveness coefficients between 300 and 360 nm than that of the 4-h BWF (Fig. 4d). However, the differences were small compared with the uncertainty in the BWFs, as reflected in the 95% confidence intervals for the absolute spectra (Fig. 4c).

BWFs were also derived using the two simpler kinetic models, the irradiance-dependent and cumulative-exposure models (Fig. 5). The shape of the BWFs did not significantly differ as a function of the kinetic model used. The results demonstrated the robustness of the PCA method for deriving

BWFs, regardless of the kinetic model used and its underlying assumptions.

The variable sensitivity, as reflected in the $\epsilon_{R(300)}$, of the different algal assemblages (Fig. 3a, Table 3) was not clearly related to community composition, as reflected in the dominant genera of nano- and microphytoplankton. For example, the algal community with the lowest overall UVR sensitivity (8 June 1998) was dominated by a small chrysophyte, whereas a community sampled the next day (9 June 1998), which was dominated by the same small chrysophyte, showed a significantly higher sensitivity (Table 3). Light availability and status may have influenced UVR sensitivity more but not in any simple way. The highest values for $\lambda_{R(300)}$ were associated with the lowest values of E_k (Table 3), which suggests greater sensitivity in more shade-adapted populations, but $\epsilon_{R(300)}$ also tended to increase with mean PAR ($P = 0.056$ for simple linear correlation).

Comparison of kinetic models (1998)—The R model accounted for 73.5%–95.7% (average, 86%) of the variance in UVR- and PAR-dependent photosynthesis (Table 3). PAR was a statistically significant contributor to the photoinhibition of primary production in only one (8 June 1998) of

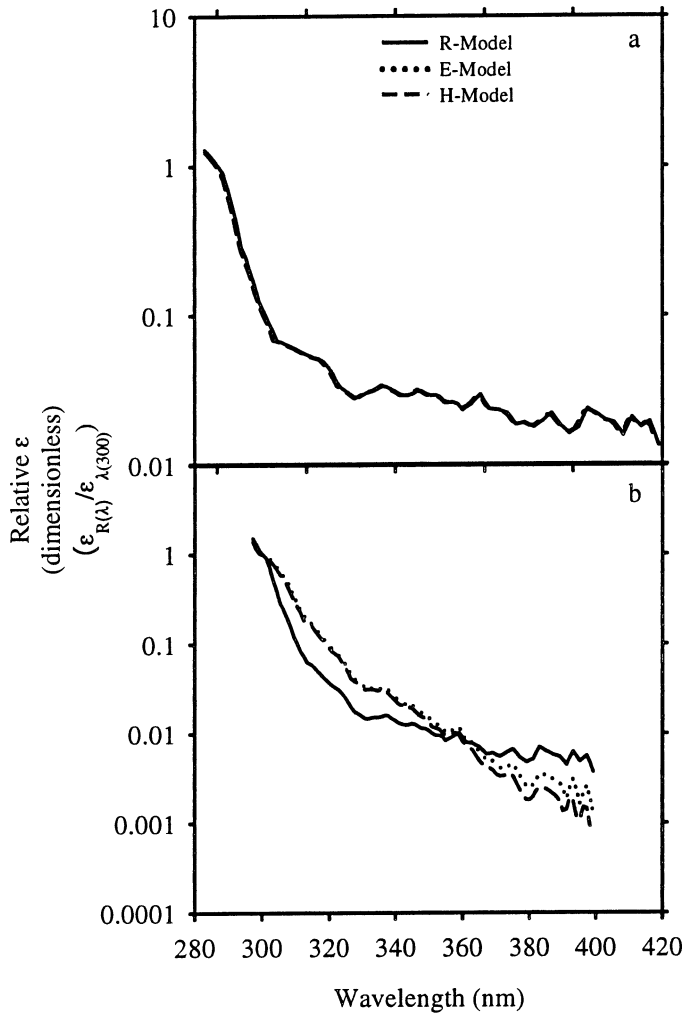


Fig. 5. Comparisons of BWFs derived using all three kinetic models for (A) 8 June and (B) 14 July 1998. Solid line: *R* model, dotted line: *E* model, dashed line: *H* model. In panel A, all three lines coincide and therefore appear to be one line.

the five 1998 experiments (i.e., ϵ_{PAR} was significantly greater than zero). The same sample showed the lowest $\epsilon_{R(300)}$ value and the lowest recovery rate constant (Table 3). On all other dates, PAR-dependent inhibition resulted in <10% inhibition (e.g., Fig. 6a). The estimated recovery rate constants ranged from not significantly different from zero (8 June 1998) to $18.25 \times 10^{-4} \text{ s}^{-1}$ (13 August 1998; Table 3).

The irradiance (*E*) and cumulative-exposure (*H*) kinetic models provided variable fits to the 1998 data. The r^2 values ranged 0.251–0.749 and 0.318–0.956 for the *E* and *H* models, respectively. Paired partial *F* tests showed that the *R* model significantly ($P < 0.000001$) improved the fit compared with the *E* and *H* models, except on 8 June 1998, when the *H* and *R* model fits were not significantly different ($P = 0.558$; $F_{1,26} = 0.35$). On that date, the estimated recovery rate constant was not significantly different from zero, which follows the assumptions of the *H* model. The *R* model was a much better predictor of the temporal variation in P_{avg}/P_{opt} compared with the *E* and *H* models (Fig. 6). The perfor-

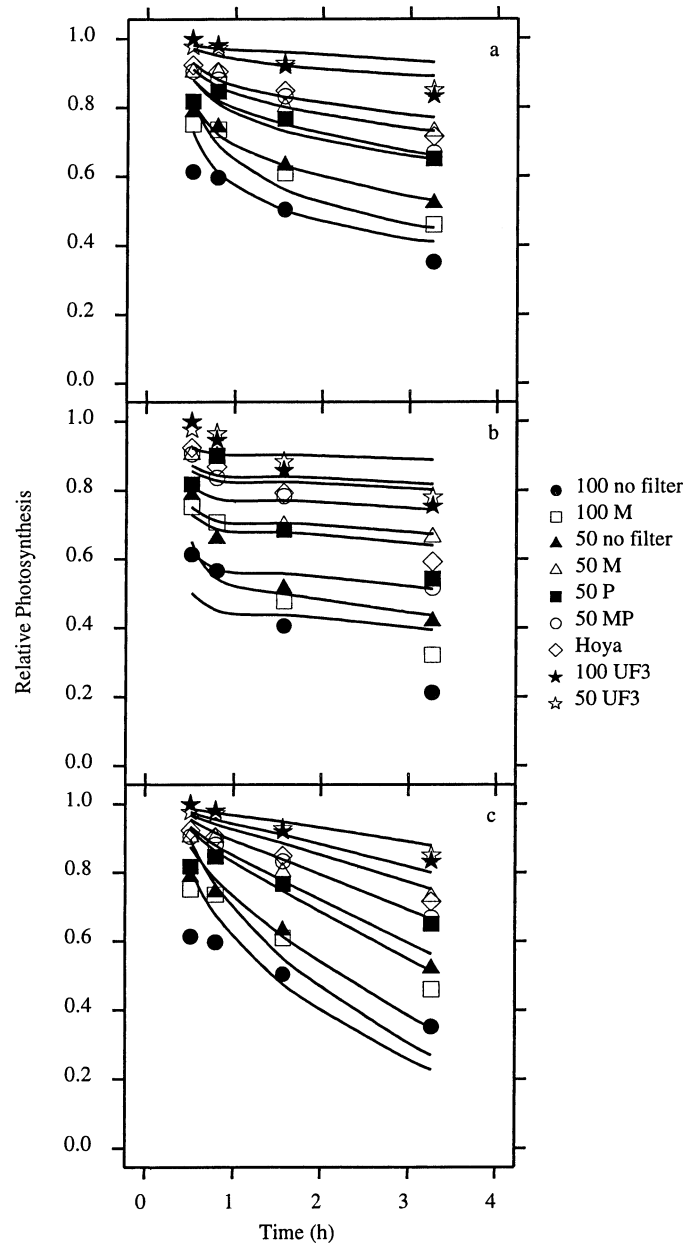


Fig. 6. Measured temporal variations in relative photosynthesis (P_{avg}/P_{opt}) on 14 July 1998 for all spectral treatments with the fitted lines for the (A) *R* model, (B) *E* model, and (C) *H* model. Values in the legend represent the level of PAR (100% or 50%). See Fig. 2 for detail on spectral filter treatments.

mance of the *E* and *H* models depended on the prevailing recovery rates, as estimated by the fitted value of k_2 in the *R* model. The variance explained by the *H* model decreased as recovery rate constants increased (Fig. 7a, $P < 0.05$), whereas that explained by the *E* model increased ($P < 0.01$). Recovery-rate constants did not correlate significantly with the light adaptation indicator (E_k), light history (% mean PAR), the light attenuation coefficient (K_d), $\epsilon_{R(300)}$, or temperature (Tables 1, 3).

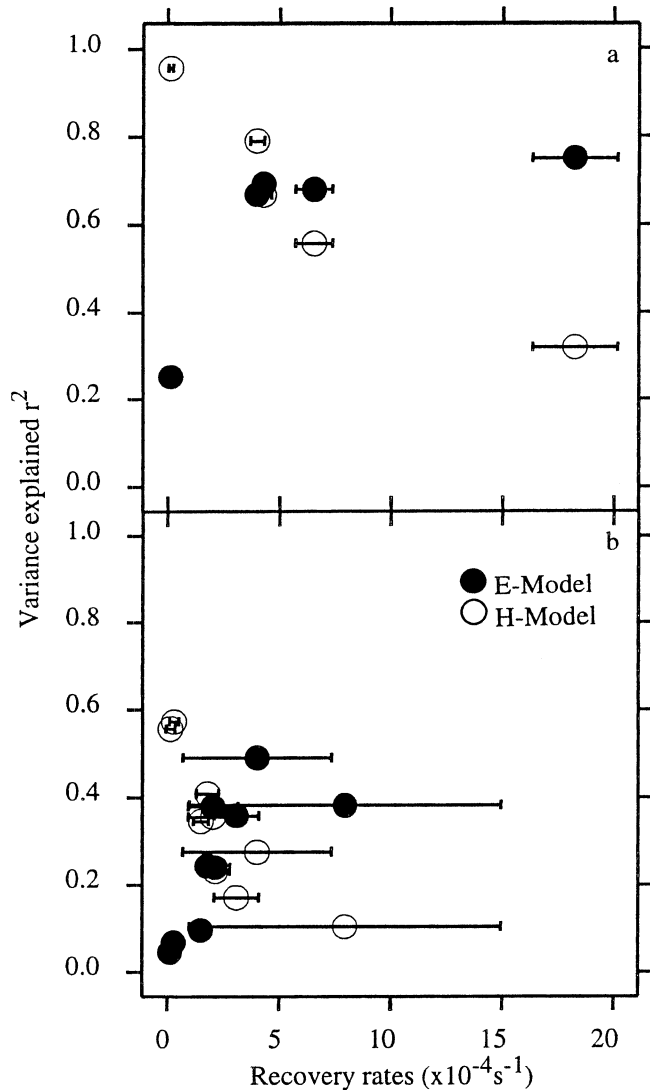


Fig. 7. Irradiance (E) and cumulative-exposure (H) model performances vs. estimated recovery rate constants (k_2 , R model) for the (A) 1998 and (B) 1997 data. Error bars represent asymptotic standard errors of the R model estimated recovery rate constants. The data value for 8 June 1998 (E model) had a high Studentized residual and was consequently deemed to be an outlier and excluded from the linear regression analysis (see "Results").

Application of models to 1997 observations—The ability of the models and the BWFs derived from the 1998 calibration experiments to predict photoinhibition in other years and stations was tested using the 1997 experimental results. An average BWF was calculated from the 1998 BWFs (excluding 13 August 1998) and used to weight the solar radiation measured in 1997. The R model could be fitted to every experiment conducted in 1997 (Table 4), but it did not perform as well as it had for 1998 data. On average, the R model accounted for 52.2% (range, 44.1%–60.8%) of the variance in UVR-dependent inhibition. This lower r^2 value does not necessarily mean that the model did not perform well. In 1997, no UF3 (total UVR) filter was used, thereby

reducing the UVR-dependent variance available to be explained by the R model. This by itself would substantially reduce the r^2 value. A visual comparison of the success of the R model in 1997 and 1998 is found in Fig. 8. Estimates of recovery rate constants ranged from 0.14 to $7.96 \times 10^{-4} \text{ s}^{-1}$. Despite the modest success of the R model, it significantly ($P < 0.05$; partial F -test) improved the proportion of variance explained compared with the E and H models in all but 2 comparisons (R vs. H model; 4 June and 2 July 1997). Once again, significant positive (E model, $P < 0.01$; $r^2 = 0.409$) and negative (H model, $P < 0.01$; $r^2 = 0.632$) linear relationships were observed between the amount of explained variation (r^2) by the E and H kinetic models and the estimated recovery rate constants in 1997 (Fig. 7b).

Integrated photoinhibition losses—Daily losses of production over a 10-m mixed layer were calculated using each kinetic model with the appropriate BWF and recovery rate constant (Table 5). Model comparisons of photoinhibition estimates for a static water column were higher than a mixing water column in all but one case (14 July, H model simulation). On all simulated dates, the E and H models predicted the lowest and highest photoinhibition estimates, and the R model predicted intermediate water column photoinhibition (Table 5). Predictions from the E and R models were within 1% of each other when estimated recovery rates were high (12 August), whereas predictions from the H and R models were within 2% of each other when estimated recovery rates were low (8 June) (Table 5). For the dates examined here, variations in integrated photoinhibition were responsive to both variations in recovery rate constants and sensitivity, defined by $\epsilon_{R(300)}$.

Discussion

The BWFs derived in the present study were, on average, consistent in their relative shape, demonstrating a rapid decrease of biological effectiveness coefficients with increasing wavelength (295–330 nm). Weighting was particularly low, relative to previously published BWFs (Cullen et al. 1992; Banaszak and Neale 2001; Neale et al. 2001a), in the 300–360 nm region. The shape of the BWF reflects the sensitivity of the biological response of interest to various wavelengths and may be indicative of prior adaptation to inhibiting radiation. To our knowledge, only one study (Neale et al. 1998a) has reported the effects of light adaptation and/or history on the shape of a BWF for UVR. The dinoflagellate *Gymnodinium sanguineum*, grown under high light, demonstrated increased concentrations of mycosporine-like amino acids (MAAs) and lower effectiveness coefficients between 320 and 340 nm. MAAs vary in the position of their absorption maxima (Garcia-Pichel and Castenholz 1993; Roy 2000) and can potentially provide protection throughout the 305–360 nm band, in which the Lake Erie BWFs were particularly low. Unfortunately, we had no direct measurements of MAAs or related pigments to verify this possibility.

The shapes of BWFs are susceptible to distortions through the interactions between different wavelengths, especially with longer exposure time (Cullen and Neale 1997; Neale 2000). Likewise, wavelength- and time-dependent repair

Table 4. Summary of the statistical analyses, done using the 1997 primary production data. The recovery rate constants (s^{-1}) were estimated by the R model, and the spectral radiation was weighted using an average BWF derived in 1998. The performance of the E and H models are listed for comparison.

Date	$k_2 \times 10^{-4}$	Model performance (r^2)			F value	
		R	E	H	R vs E	R vs H
7 May 1997	2.04 ± 1.39	0.502	0.379	0.355	40.6 _{1,29}	8.6 _{1,29}
3 Jun 1997	4.01 ± 3.07	0.562	0.490	0.275	46.1 _{1,30}	19.5 _{1,30}
4 Jun 1997	0.30 ± 0.35	0.583	0.067	0.572	129.7 _{1,34}	0.9 _{1,34}
5 Jun 1997	2.15 ± 1.12	0.457	0.240	0.231	64.6 _{1,34}	14.1 _{1,34}
2 Jul 1997	0.14 ± 0.30	0.558	0.045	0.556	138.6 _{1,34}	0.2 _{1,34}
29 Jul 1997	7.96 ± 6.26	0.441	0.382	0.103	56.8 _{1,34}	20.6 _{1,34}
30 Jul 1997	1.79 ± 0.76	0.608	0.243	0.408	120.1 _{1,34}	17.4 _{1,34}
31 Jul 1997	3.09 ± 1.50	0.498	0.358	0.171	57.7 _{1,34}	22.2 _{1,34}
27 Aug 1997	1.38 ± 0.67	0.490	0.095	0.345	104.0 _{1,34}	9.7 _{1,34}

processes (e.g., Mitchell and Karentz 1993) may also contribute to variations in BWF shapes. Our experimental protocols involved longer incubations and greater exposure to PAR and long-wavelength UVA than those used to produce most previously published BWFs (e.g., Cullen et al. 1992; Neale 2000). However, the BWFs derived from short (≤ 1 h) exposures had similarly low coefficients in the 305–360 nm range as those from long (≤ 4 h) exposures. The choice of kinetic model also made little difference in the shape of the estimated BWF. These results suggest that the lower effectiveness coefficients between 305 and 360 nm were real observations and not artifacts of the length of our exposures or of our assumptions about the kinetics of inhibition.

The three kinetic models tested here varied in their ability

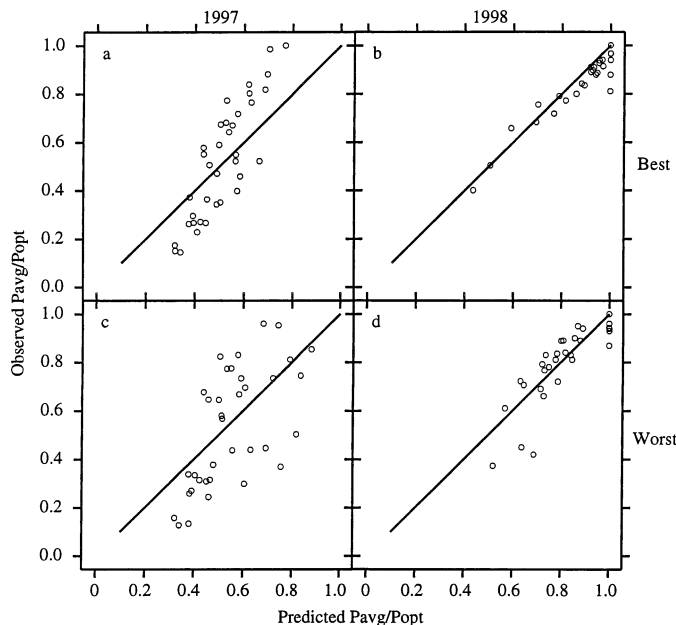


Fig. 8. Observed vs. R model predicted values for both 1997 and 1998, depicting model performance range in each year. (A, B) Best goodness-of-fit data observed for 30 July 1997 ($r^2 = 0.608$) and 8 June 1998 ($r^2 = 0.957$), respectively. (C, D) Worst goodness-of-fit data observed for 29 July 1997 ($r^2 = 0.441$) and 12 August 1998 ($r^2 = 0.735$), respectively. Solid line represents the 1:1 line.

to predict UVR- and PAR-dependent photoinhibition in Lake Erie phytoplankton, but the R model was consistently the better predictor. The cumulative-exposure (H) model has successfully described the responses of natural communities in cold waters of the Southern Ocean (Neale et al. 1998b,c) and in both cold (springtime) and warm (summertime) waters of Lake Ontario (Smith et al. 1998), although the latter study used predefined BWFs from studies of marine phytoplankton. The E model has shown broader success with marine, estuarine, and freshwater phytoplankton (e.g., Neale and Kieber 2000; Köhler et al. 2001). However, neither the E nor the H model was consistently satisfactory for Lake Erie phytoplankton in either 1997 or 1998. The relative success of the R model, the nonzero recovery rates it usually indicated, and their relationship to the E and H model performances (in terms of r^2) supported the idea that slow rates of recovery have a significant influence on the UVR-dependent response of Lake Erie phytoplankton. Additionally, compared with other studies, the R model presented here seemed to return reasonable estimates of recovery rates. Héraud and Beardall (2000) investigated the recovery of photosynthetic performance (fluorescence parameters) in *Dunaliella tertiolecta* and calculated rates of recovery ranging $0.67\text{--}2.0 \times 10^{-4} s^{-1}$, whereas Litchman et al. (2002) estimated average rates of recovery of 12.7 and $20 \times 10^{-4} s^{-1}$, respectively, for nitrogen-deficient and -sufficient cultures of marine dinoflagellates. The recovery rate estimates from our study span the entire spectrum of estimates from these studies ranging $0.14\text{--}18.25 \times 10^{-4} s^{-1}$.

Lake Erie phytoplankton previously exposed to full spectrum sunlight can achieve near-complete recovery of photosynthetic electron transport within 2 h under dim light conditions (Marwood et al. 2000), which is consistent with the active recovery processes inferred from our results. The median recovery rate constant for our 1998 experiments ($\sim 1.5 h^{-1}$) would predict 90% recovery within 2 h in nonphoto-inhibiting conditions, even for populations reduced to 10% of their normal (noninhibited) photosynthetic performance. Such rapid recovery would suggest an important role for short-term defense mechanisms such as energy dissipation via fluorescence (Ferris and Christian 1991) or the repair of rapidly cycled components such as the D1 protein of pho-

Table 5. Integrated water column inhibition estimates, calculated using the 8 June, 14 July, and 12 August 1998 BWFs, and for all three kinetic models (*R*, *E*, and *H*). The estimates were computed using the actual values of P_m^b , α^b , and k_2 (s^{-1}) derived from each phytoplankton assemblage, as well as the BWFs specific to each date and model. Estimates were calculated for a static and a mixed water column. Mixing rates are expressed as radial velocity.

BWF	$\varepsilon_{R(300)}$ $\times 10^{-4}$	$k_2 \times 10^{-4}$	Integrated inhibition (%)								
			Static			5 h cycle ⁻¹			0.5 h cycle ⁻¹		
			<i>R</i>	<i>E</i>	<i>H</i>	<i>R</i>	<i>E</i>	<i>H</i>	<i>R</i>	<i>E</i>	<i>H</i>
8 Jun 1998	1.08	0.14	7.0	0.9	8.7	4.0	0.8	5.3	3.9	0.8	5.2
14 Jul 1998	16.1	3.99	13.3	2.6	24.3	11.6	2.3	26.4	11.4	2.3	26.8
12 Aug 1998	1.41	6.54	1.7	1.5	8.4	1.6	1.4	5.6	1.6	1.4	5.5

tosystem II (Greenberg et al. 1989). Recovery was not always so rapid, however, which possibly reflects longer-lasting damage (e.g., structural damage to membranes, enzymes, or nucleic acids), which would require lengthier recovery times (Mitchell and Karentz 1993; Vincent and Neale 2000).

The variability of both sensitivity, as reflected in BWF coefficients, and recovery rate constants suggests the possibility of alternative strategies to minimize UVR damage. For example, the phytoplankton communities of 8 June and 12 August 1998 both showed low ε_{R300} values but very different recovery rate constants. We were unable to explain the variations in recovery rate constants with our measures of light availability, photoadaptive state, or temperature, even with the addition of the more numerous (albeit less reliable) estimates obtained by extrapolating the 1998 BWFs to 1997 (Table 4). The nutrient supply, particularly of nitrogen, might be expected to constrain the potential for some types of repair activity (e.g., Lesser et al. 1994). Physiological indices of phosphorus and nitrogen status were used in 1997 to characterize each sample as either deficient or not with respect to each nutrient (Hiriart et al. 2002). This too failed to explain the variations, with N-limited samples (7 May, 5 June, and 30 July 1997) and P-limited samples (3 June and 2, 30, and 31 July 1997) having recovery rate constants distributed around the overall median value (Table 4). Other aspects of the nutrient and light regime or of community taxonomic composition may be responsible, but we cannot currently explain the variations in recovery rates.

The integrated loss of production due to photoinhibition was modeled for three samples with contrasting sensitivity ($\lambda_{R(300)}$) and recovery (k_2) attributes using all three kinetic models. Under these scenarios, the *R* model estimates were systematically intermediate between the *E* and *H* model predictions, as had been expected from the underlying assumptions of each model. In all cases, recovery was likely active but was not fast enough to establish instantaneous equilibrium with damage; some cumulative effects of UVR exposure may also have occurred, which are considered to be negligible by the *E* model. Although it seems likely that the *E* model is not fully accurate for some phytoplankton communities, it did provide, on average, integrated photoinhibitory loss estimates within 5% of those obtained with the more complicated *R* model, particularly in the mixed-water column simulations (Table 5). This was true even though we included a sample with an extremely low recovery rate constant. On average, mixing of the water column conferred

some protection from UVR exposure, a fact reflected in the reduced integrated photoinhibition estimates. This protection was greatest on 8 June and smallest on 12 August, which indicates the importance of UVR refuges—water column depth—for algal populations with lower recovery rates.

Few studies have investigated the impact of mixing on UVR-dependent photoinhibition, particularly in freshwater ecosystems. UVR-dependent inhibition (UVB and part of UVA) of carbon assimilation rates ranging 10%–30% have been reported for a 10-m mixed water column in a freshwater lake (Köhler et al. 2001). By comparison, integrated losses to inhibition in a temperate zone estuary range 3%–33% (Neale 2001), whereas estimates for phytoplankton in the Southern Ocean range 5%–50%, depending on many assumptions about mixing and radiation regime (Neale et al. 1998c). The integrated inhibition estimates that we made fall within the range of estimates for natural phytoplankton communities but were designed only to provide comparisons between models under standardized assumptions of spectral transmission, mixing depth, and mixing rates. More realistic estimates for Lake Erie will require accounting for the variability of such modifying factors as well as diurnal/temporary near-surface thermoclines, which can be important determinants of UVR exposure (Milot-Roy and Vincent 1994).

References

- BANASZAK, A. T., AND P. J. NEALE. 2001. Ultraviolet radiation sensitivity of photosynthesis in phytoplankton from an estuarine environment. *Limnol. Oceanogr.* **46**: 592–603.
- BEHRENFELD, M. J., J. W. CHAPMAN, J. T. HARDY, AND H. LEE II. 1993. Is there a common response to ultraviolet-B radiation by marine phytoplankton? *Mar. Ecol. Prog. Ser.* **102**: 59–68.
- BOUCHER, N. P., AND B. B. PRÉZELIN. 1996. Spectral modeling of UV inhibition of in situ Antarctic primary production using a field-derived biological weighting function. *Photochem. Photobiol.* **64**: 407–418.
- CHARLTON, M. N., R. LESAGE, AND J. E. MILNE. 1999. Lake Erie in transition: The 1990's, p. 97–124. *In* M. Munawar, T. A. Edsall, and I. F. Munawar [eds.], *The state of Lake Erie (SOLE)—past, present and future*. Backhuys.
- COOHILL, T. P. 1997. UV action spectra for marine phytoplankton. *Photochem. Photobiol.* **65**: 259–260.
- CULLEN, J. J., AND M. P. LESSER. 1991. Inhibition of photosynthesis by ultraviolet radiation as a function of dose and dosage rate: Results for a marine diatom. *Mar. Biol.* **111**: 183–190.
- , AND P. J. NEALE. 1997. Biological weighting functions for

- describing the effects of ultraviolet radiation on aquatic systems, p. 97–118. In D.-P. Häder [ed.], *The effects of ozone depletion on aquatic ecosystems*. R. G. Landes.
- , ———, AND M. P. LESSER. 1992. Biological weighting function for the inhibition of phytoplankton photosynthesis by ultraviolet radiation. *Science* **258**: 646–650.
- FERRIS, J. M., AND R. CHRISTIAN. 1991. Aquatic primary production in relation to microalgal responses to changing light: A review. *Aquat. Sci.* **53**: 187–217.
- GARCIA-PICHEL, F., AND R. W. CASTENHOLZ. 1993. Occurrence of UV-absorbing, mycosporine-like, compounds among cyanobacterial isolates, and an estimate of their screening capacity. *Appl. Environ. Microbiol.* **59**: 163–169.
- GREENBERG, B. M., V. GABA, O. CANAANI, S. MALKIN, A. K. MATTOO, AND M. EDELMAN. 1989. Separate photosensitizers mediate degradation of the 32-kDa photosystem II reaction center protein in the visible and UV spectral regions. *Proc. Natl. Acad. Sci. USA* **86**: 6617–6620.
- HERAUD, P., AND J. BEARDALL. 2000. Changes in chlorophyll fluorescence during exposure of *Dunaliella tertiolecta* to UV radiation indicate a dynamic interaction between damage and repair processes. *Photosynth. Res.* **63**: 123–134.
- HERRMANN, H., D.-P. HÄDER, AND F. GHETTI. 1997. Inhibition of photosynthesis by solar radiation in *Dunaliella salina*: Relative efficiencies of UV-B, UV-A and PAR. *Plant Cell Environ.* **20**: 359–365.
- HIRIART, V. P., B. M. GREENBERG, S. J. GUILDFORD, AND R. E. H. SMITH. 2002. Effects of ultraviolet radiation on rates and size distribution of primary production by Lake Erie phytoplankton. *Can. J. Fish. Aquat. Sci.* **59**: 317–328.
- KARENTZ, D. 1999. Evolution and ultraviolet light tolerance in algae. *J. Phycol.* **35**: 629–630.
- , J. E. CLEAVER, AND D. L. MITCHELL. 1991. Cell survival characteristics and molecular responses of Antarctic phytoplankton to ultraviolet-B radiation. *J. Phycol.* **27**: 326–341.
- KÖHLER, J., M. SCHMITT, H. KRUMBECK, M. KAPFER, E. LITCHMAN, AND P. J. NEALE. 2001. Effects of UV on carbon assimilation of phytoplankton in a mixed water column. *Aquat. Sci.* **63**: 294–309.
- LESSER, M. P., J. J. CULLEN, AND P. J. NEALE. 1994. Carbon uptake in a marine diatom during acute exposure to ultraviolet B radiation: Relative importance of damage and repair. *J. Phycol.* **30**: 183–192.
- LITCHMAN, E., P. J. NEALE, AND A. T. BANASZAK. 2002. Increased sensitivity to ultraviolet radiation in nitrogen-limited dinoflagellates: Photoprotection and repair. *Limnol. Oceanogr.* **47**: 86–94.
- MARWOOD, C. A., R. E. H. SMITH, J. A. FURGAL, M. N. CHARLTON, K. R. SOLOMON, AND B. M. GREENBERG. 2000. Photoinhibition of natural phytoplankton populations in Lake Erie exposed to solar ultraviolet radiation. *Can. J. Fish. Aquat. Sci.* **57**: 371–379.
- MILOT-ROY, V., AND W. F. VINCENT. 1994. UV radiation effects on photosynthesis: The importance of near-surface thermoclines in a subarctic lake. *Arch. Hydrobiol. Beig. Ergebn. Limnol.* **43**: 171–184.
- MITCHELL, D. L., AND D. KARENTZ. 1993. The induction and repair of DNA photodamage in the environment, p. 345–377. In A. R. Young, et al. [eds.], *Environmental UV photobiology*. Plenum Press.
- NEALE, P. J. 2000. Spectral weighting functions for quantifying effects of UV radiation in marine ecosystems, p. 72–100. In S. J. De Mora, S. Demers, and M. Vernet [eds.], *The effects of UV radiation in the marine environment*. Cambridge Univ. Press.
- . 2001. Effects of ultraviolet radiation on estuarine phytoplankton production: Impact of variations in exposure and sensitivity to inhibition. *J. Photochem. Photobiol. B* **62**: 1–8.
- , A. T. BANASZAK, AND C. R. JARRIEL. 1998a. Ultraviolet sunscreens in *Gymnodinium sanguineum* (Dinophyceae): Mycosporine-like amino acids protect against inhibition of photosynthesis. *J. Phycol.* **34**: 928–938.
- , J. J. CULLEN, AND R. F. DAVIS. 1998b. Inhibition of marine photosynthesis by ultraviolet radiation: Variable sensitivity of phytoplankton in the Weddell-Scotia Confluence during the austral spring. *Limnol. Oceanogr.* **43**: 433–448.
- , R. F. DAVIS, AND J. J. CULLEN. 1998c. Interactive effects of ozone depletion and vertical mixing on photosynthesis of Antarctic phytoplankton. *Nature* **392**: 585–589.
- , J. J. FRITZ, AND R. F. DAVIS. 2001a. Effects of UV on photosynthesis of Antarctic phytoplankton: Models and application to coastal and pelagic assemblages. *Rev. Chil. Hist. Nat.* **74**: 283–292.
- , AND D. J. KIEBER. 2000. Assessing biological and chemical effects of UV in the marine environment: Spectral weighting functions, p. 61–83. In R. E. Hester and R. M. Harrison [eds.], *Causes and environmental consequences of increase UV-B radiation*. Issues in Environmental Science and Technology 14. Royal Society of Chemistry.
- , AND OTHERS. 2001b. Quantifying the response of phytoplankton photosynthesis to ultraviolet radiation: Biological weighting functions versus in situ measurements in two Swiss lakes. *Aquat. Sci.* **63**: 265–285.
- PIENITZ, R., AND W. F. VINCENT. 2000. Effect of climate change relative to ozone depletion on UV exposure in subarctic lakes. *Nature* **404**: 484–487.
- PLATT, T., C. L. GALLEGOS, AND W. G. HARRISON. 1980. Photo-inhibition of photosynthesis in natural assemblages of marine phytoplankton. *J. Mar. Res.* **38**: 687–701.
- PRÉZELIN, B. B., N. P. BOUCHER, AND O. SCHOFIELD. 1994. Evaluation of field studies of UVB radiation effects on Antarctic marine primary productivity, p. 181–194. In R. H. Biggs and M. E. B. Joyner [eds.], *Stratospheric ozone depletion/UV-B radiation in the biosphere*. Springer-Verlag.
- ROY, S. 2000. Strategies for the minimisation of UV-induced damage, p. 177–205. In S. J. De Mora, S. Demers, and M. Vernet [eds.], *The effects of UV radiation in the marine environment*. Cambridge Univ. Press.
- SMITH, R. C., AND J. J. CULLEN. 1995. Effects of UV radiation on phytoplankton. *Rev. Geophys.* **33**: 1211–1223.
- , AND OTHERS. 1992. Ozone depletion: Ultraviolet radiation and phytoplankton biology in Antarctic waters. *Science* **255**: 953–959.
- SMITH, R. E. H., J. A. FURGAL, M. N. CHARLTON, B. M. GREENBERG, V. HIRIART, AND C. MARWOOD. 1999. The attenuation of ultraviolet radiation in a large lake with low dissolved organic matter concentrations. *Can. J. Fish. Aquat. Sci.* **56**: 1351–1361.
- , ———, AND D. R. S. LEAN. 1998. The short-term effects of solar ultraviolet radiation on phytoplankton photosynthesis and photosynthate allocation under contrasting mixing regimes in Lake Ontario. *J. Great Lakes Res.* **24**: 427–441.
- VILLAFANE, V. E., E. W. HELBLING, O. HOLM-HANSEN, AND B. E. CHALKER. 1995. Acclimatization of Antarctic natural phytoplankton assemblages when exposed to solar ultraviolet radiation. *J. Plankton Res.* **17**: 2295–2306.

- VINCENT, W. F., AND P. J. NEALE. 2000. Mechanisms of UV damage to aquatic organisms, p. 149–176. *In* S. J. De Mora, S. Demers, and M. Vernet [eds.], *The effects of UV radiation in the marine environment*. Cambridge Univ. Press.
- WILSON, M. I., AND OTHERS. 1995. In vivo photomodification of ribulose-1,5-bisphosphate carboxylase/oxygenase holoenzyme by ultraviolet-B radiation. *Plant Physiol.* **109**: 221–229.
- XIONG, F., J. KOMENDA, J. KOPECKY, AND L. NEDBAL. 1997. Strategies of ultraviolet-B protection in microscopic algae. *Physiol. Plant* **100**: 378–388.

Received: 7 November 2002

Accepted: 22 July 2003

Amended: 9 September 2003